Construction and Building Materials 107 (2016) 203–215

Contents lists available at ScienceDirect

Construction and Building Materials

journal homepage: www.elsevier.com/locate/conbuildmat

Impact resistance of a sustainable Ultra-High Performance Fibre Reinforced Concrete (UHPFRC) under pendulum impact loadings

R. Yu [a,b], L. van Beers [b], P. Spiesz [b,c], H.J.H. Brouwers [b,*]

[a] State Key Lab of Silicate Materials for Architectures, Wuhan University of Technology, Wuhan 430070, PR China
[b] Department of the Built Environment, Eindhoven University of Technology, The Netherlands
[c] ENCI HeidelbergCement Benelux, The Netherlands

HIGHLIGHTS

- A sustainable UHPFRC is developed based on particle packing model.
- A modified pendulum impact set-up is designed and produced.
- Impact resistance of UHPFRC under pendulum impact is investigated.
- The results obtained from different impact set-up are compared.
- Mechanism of the impact process is studied and discussed.

ARTICLE INFO

Article history:
Received 24 September 2015
Received in revised form 30 November 2015
Accepted 22 December 2015

Keywords:
Impact resistance
Sustainable
Ultra-High Performance Fibre Reinforced Concrete (UHPFRC)
Pendulum impact
Energy dissipation

ABSTRACT

This paper presents the impact resistance of a sustainable UHPFRC member under pendulum impact loadings. The modified Andreasen and Andersen model is employed for the concrete matrix design, and two pendulum impact set-ups are utilized in the experiments: "Charpy Impact Device" and "Modified Pendulum Impact Device". For the Charpy impact test, the obtained results show that the fibre length plays a dominating role in improving the energy dissipation capacity of the sustainable UHPFRC. With a constant total steel fibre amount, a higher proportion of short straight fibres decrease the energy absorption capacity of the concrete sample. However, the results obtained from the "Modified Pendulum Impact Device" demonstrate that, compared to the concrete with single sized fibres, the addition of hybrid steel fibres is more beneficial for improving the energy dissipation capacity of the sustainable UHPFRC under pendulum impact. Subsequently, the inconsistent results obtained from both investigated test methods are analysed and discussed. Based on the obtained experimental results, it can be concluded that there is an urgent need for a systematic standard for evaluating the impact resistance of UHPFRC.

1. Introduction

Since the beginning of the last century, due to civil safety and military purposes, the dynamic properties of concrete based materials under impact loadings have attracted much attention of researchers [1–3]. Nevertheless, as commonly known, both normal and high strength concretes are brittle, where the degree of brittleness increases as their strength increases. The conventional method to strengthen concrete against impact loading is by using continuous steel reinforcement bars (re-bars). The steel re-bars are effective in preventing the mass separation of the concrete target, keeping it intact and maintaining the structural integrity [4]. Nevertheless, with the development of the concrete industry, this approach was demonstrated to be ineffective in reducing penetration depth under projectile impact [5,6]. Therefore, some other methods were proposed to improve the energy dissipation capacity of concrete in recent decades. According to the outcome from the available literature [7–11], a strong concrete matrix and a large amount of steel fibres are beneficial for improving the impact resistance capacity of the concrete, since the damage of concrete matrix and pullout of steel fibres can absorb a large quantity of energy released during the impact process. Nowadays, with the development of concrete and chemical admixtures, a series of new materials (advanced superplasticizers, nanosilica, etc.) can be utilized to produce concrete with superior properties. Not only new materials but also new insights into the particle packing and the influence of the particle packing on the mechanical properties allowed the

* Corresponding author.
E-mail address: jos.brouwers@tue.nl (H.J.H. Brouwers).

http://dx.doi.org/10.1016/j.conbuildmat.2015.12.157
0950-0618/

Nomenclature

List of symbols

D	particle size (μm)
D_{AB}	distance between A and B (as shown in Fig. 12) (cm)
D_{CD}	distance between C and D (as shown in Fig. 12) (cm)
$D_{camera-hammer}$	distance between camera and hammer (cm)
$D_{camera-board}$	distance between the camera and the mesh board (cm)
D_{max}	maximum particle size (μm)
D_{min}	minimum particle size (μm)
$E_{absorbed}$	absorbed energy by the sustainable UHPFRC slab (J)
E_{loss}	energy loss amount during the hammer swing process (J)
$E_{total-absorbed}$	total absorbed energy by the sustainable UHPFRC slab (J)
g	gravity of earth constant (9.81) (m/s^2)
h_{hammer}	maximum height of the hammer (m)
M_{hammer}	mass of impact hammer (kg)
M_{slab}	mass of concrete slab (kg)
n	shock numbers when entire damage of concrete slab happens (−)
P_{mix}	composed mix (−)
P_{tar}	target curve (−)
$P(D)$	a fraction of the total solids being smaller than size D (−)
q	distribution modulus (−)
R^2	coefficient of determination (−)
RSS	sum of the squares of the residuals (−)
V_{hammer}	initial impact velocity of the hammer (m/s)
$V_{hammer-residual}$	slab velocity after impact (m/s)
V_{slab}	residual velocity of hammer after the impact (m/s)
V_{tested}	tested hammer impact velocity (m/s)
$V_{theoretical}$	hammer theoretical impact velocity (m/s)

design of concrete mixes that have higher strength and deformation capacity than normal strength concrete (NSC). Considering the requirements of a strong concrete matrix and a large amount of steel fibres, the newly developed (at the beginning of 1990s) ultra-high performance fibre-reinforced concrete (UHPFRC) could be a good candidate to be utilized in protective structures.

Ultra-High Performance Fibre Reinforced Concrete (UHPFRC) is a relatively new construction material, which is a combination of high performance concrete matrix and fibre reinforcement [12]. It can be treated as a combination of three concrete technologies to a greater extent: self-compacting concretes (SCC), fibre reinforced concretes (FRC) and high performance concretes (HPC) [13]. Due to the relatively high binder content, low water to binder ratio and high fibre dosage, UHPFRC has superior mechanical properties and energy absorption capacity [14–16]. The stress–strain curves depicted in Fig. 1 clearly show that the energy adsorbed by UHPFRC in straining is extensive. The consumed energy is represented by the area under the stress–strain curve. This high potential of energy absorption capacity makes UHPFRC suitable for applications where high energy is released. This is the case for all mechanical impact loads acting on structural members. These impact loads can be caused by: (1) vehicle impacts, (2) deflagration of inflammable chemicals, (3) detonation of explosives and (4) ballistic impacts. Here, UHPFRC can be used for strengthening and protection of already existing buildings or the design of new structural members.

In the available literature, several investigations regarding dynamic performance of UHPFRC under different types of impact can be found. For example, Bindiganavile et al. [7] demonstrated that UHPFRC has higher impact resistance than other types of concretes. Their impact tests were carried out with a 60 kg drop-mass, hitting a variable span beam specimen from heights of up to 2.5 m. To cover a large range of loading rates, Parant et al. [9] employed two dynamic impact tests using a four-point bending set-up on thin UHPFRC slabs with three quasi-static loading rates (3.3×10^{-6}, 3.3×10^{-4} and 3.3×10^{-3} s^{-1}) and a block-bar device with a bar velocity of 5.55 m/s. Their results showed that with an increase in the strain rate, the modulus of rupture and the uniaxial tensile strength increase. Habel and Gauvreau [10] presented an experimental and analytical study of the load rate-dependent characteristics of UHPFRC. The obtained results showed a significantly increased strength and fracture energy of the dynamically loaded plates when compared to quasi-static loading. Lai and Sun [11] studied the dynamic behaviour of UHPFRC with different steel fibre volume fractions under impact using the split Hopkinson pressure bar device. It was proven that, at high strain rates, the unreinforced specimens fracture into small parts while the fibre reinforced ones only have fine cracks on the edges. Máca et al. [18] and Sovják et al. [19] investigated the impact resistance of UHPFRC against bullets fired. It was experimentally verified that the optimal fibre content in the UHPFRC mixture is 2% by volume. No improvement in all damage parameters was observed when the fibre volume fraction

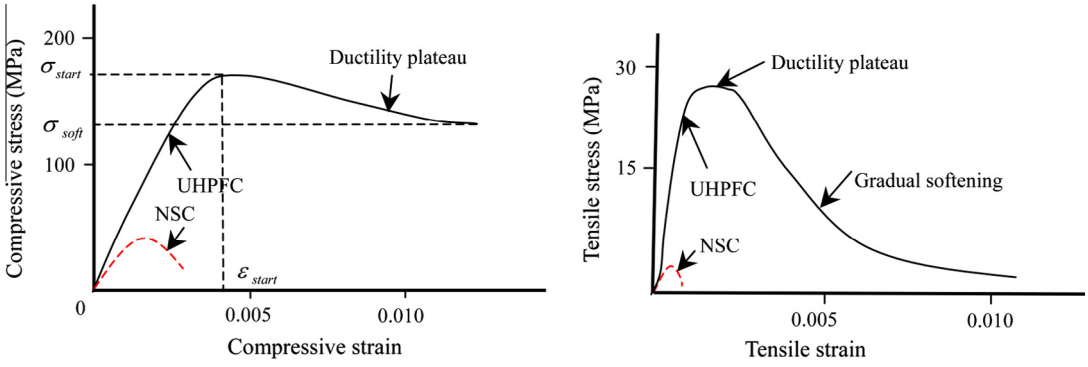

Fig. 1. Mechanical properties of conventional concrete and UHPFRC under compressive load (left) and tensile load (right) [17].

Fig. 2. Steel fibres used in this study.

Table 1
Information of materials used.

Materials	Type	Specific density (kg/m^3)
Cement	CEM I 52.5 R	3150
Filler	Limestone powder	2710
Fine sand	Microsand	2720
Coarse sand	Sand 0–2	2640
Superplasticizer	Polycarboxylate ether	1050
Pozzolanic material	Nano-silica (nS)	2200
Fibre-1	Long straight steel fibre (13/0.2)	7800
Fibre-2	Short straight steel fibre (6/0.16)	7800
Fibre-3	Hook ended steel fibre (35/0.55)	7800

Table 2
Oxide composition of employed cement, limestone powder and nano-silica.

Substance	Cement (mass%)	Limestone powder (mass%)	Nano-silica (mass%)
CaO	64.60	89.56	0.08
SiO_2	20.08	4.36	98.68
Al_2O_3	4.98	1.00	0.37
Fe_2O_3	3.24	1.60	–
K_2O	0.53	0.34	0.35
Na_2O	0.27	0.21	0.32
SO_3	3.13	–	–
MgO	1.98	1.01	–
TiO_2	0.30	0.06	0.01
Mn_3O_4	0.10	1.605	–
P_2O_5	0.74	0.241	0.15
Cl^-	0.05	–	0.04

was increased from 2% to 2.5% or 3%. Similarly to that, Wu et al. [20] investigated the impact resistance of UHPFRC under projectile impact with the velocity of 510–1320 m/s. The experimental results confirmed that UHPFRC has excellent projectile impact resistance, by reducing the depth of penetration and the crater dimensions of the rigid projectile, as well as by deforming and deviating the terminal ballistic trajectory of the abrasive projectile. However, it can be noticed that all these tested UHPFRCs are normally produced with a large amount of cement or binders, which is not in line with the sustainable development concept and sometimes limits its wider application. In the authors' previous research [21–24], it has been demonstrated how to produce a UHPFRC with relatively low cement amount, mineral admixture and an optimized particle packing, employing modified Andreasen and Andersen particle packing model. Moreover, it is demonstrated that this developed UHPFRC has a reduced environmental impact compared to the conventional UHPFRCs. However, the research focusing on impact resistance of the sustainable UHPFRC is scarce, and it is unclear whether such UHPFRC would be sufficient for protection purposes.

Consequently, based on the premises mentioned above, the objective of this study is to investigate the impact resistance of the developed sustainable UHPFRC under pendulum impact loadings. The design of concrete mixture aims to achieve a densely compacted cementitious matrix with a relatively low cement amount with mineral admixtures and with the composition optimized, by applying the modified Andreasen and Andersen particle packing model. In addition, two types of pendulum impact set-ups are employed to evaluate the impact resistance of the sustainable UHPFRC.

2. Materials and methods

2.1. Materials

The cement used in this study is Ordinary Portland Cement (OPC) CEM I 52.5 R, provided by ENCI HeidelbergCement (the Netherlands). A polycarboxylic ether based superplasticizer is used to adjust the workability of concrete. Limestone powder is used as a filler to replace cement. A commercially available nano-silica in slurry is applied as a pozzolanic material. Two types of sand are used, one is a river dredged sand in the fraction of 0–2 mm and the other one is a microsand in the 0–1 mm size range (Graniet-Import Benelux, the Netherlands). Additionally, three

Table 3
Recipes of the developed sustainable UHPFRC.

No.	OPC kg/m^3	LP kg/m^3	MS kg/m^3	*S* kg/m^3	nS kg/m^3	*W* kg/m^3	SP kg/m^3	LSF vol.%	SSF vol.%	HF vol.%
1	594.2	265.3	221.1	1061.2	24.8	176.9	44.2	0	0	0
2	594.2	265.3	221.1	1061.2	24.8	176.9	44.2	2.0	0	0
3	594.2	265.3	221.1	1061.2	24.8	176.9	44.2	1.5	0.5	0
4	594.2	265.3	221.1	1061.2	24.8	176.9	44.2	1.0	1.0	0
5	594.2	265.3	221.1	1061.2	24.8	176.9	44.2	0.5	1.5	0
6	594.2	265.3	221.1	1061.2	24.8	176.9	44.2	0	2.0	0
7	594.2	265.3	221.1	1061.2	24.8	176.9	44.2	0.5	0	1.5
8	594.2	265.3	221.1	1061.2	24.8	176.9	44.2	0	0	2

OPC: cement, LP: limestone powder, M-S: microsand, N-S: normal sand, nS: nano-silica, W: water, SP: superplasticizer, LSF: long straight fibre, SSF: short straight fibre, HF: hook ended fibre, Ref.: reference sample without fibres.

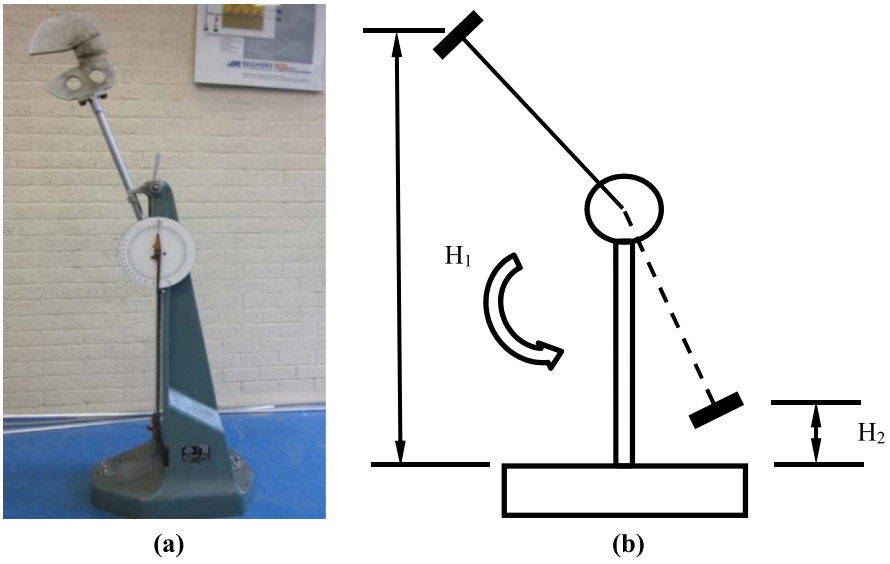

Fig. 3. "Charpy Impact Device" used in this study (a) and its working scheme (b).

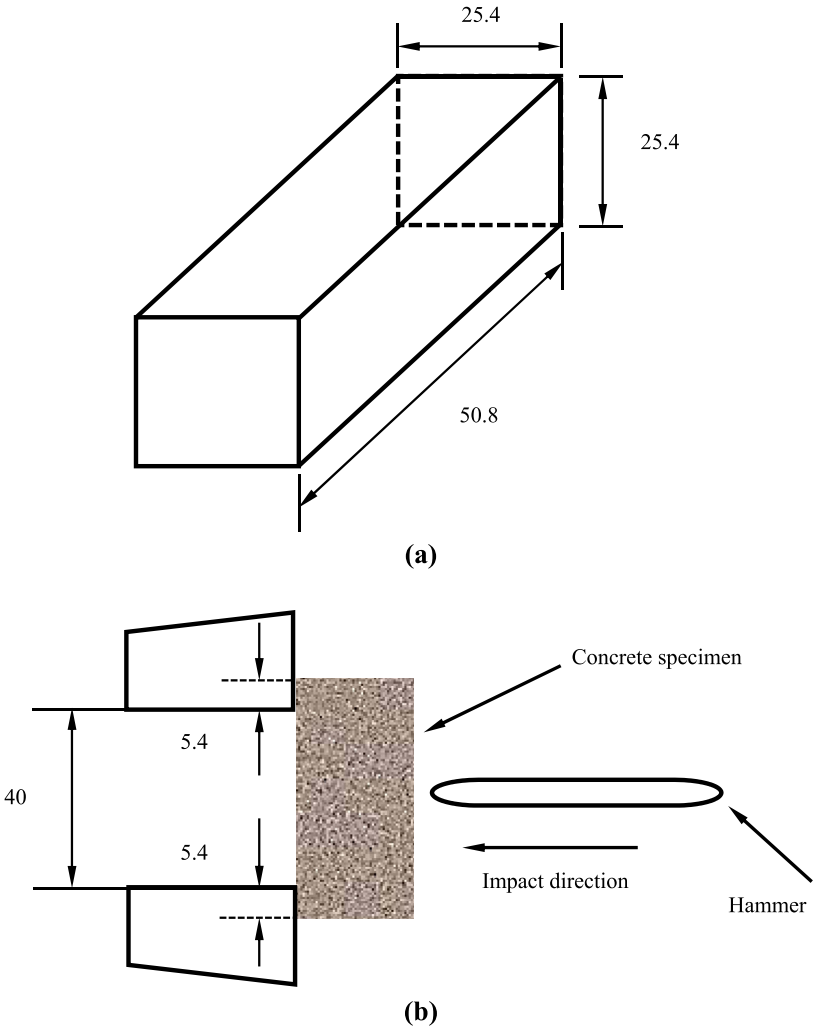

Fig. 4. Dimensions of sample for Charpy impact test (a) and configuration of its impact loading process (b) (units: mm).

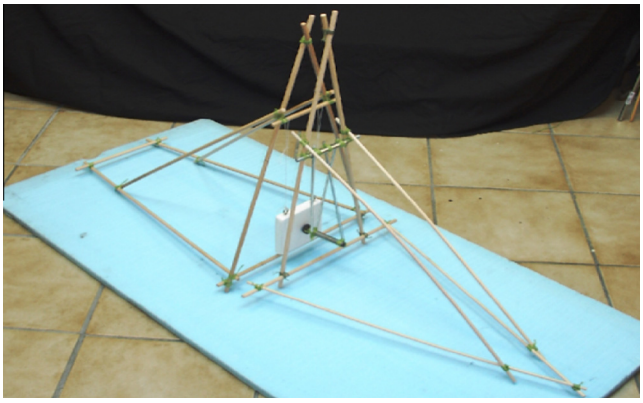

Fig. 5. Model of the "Modified Pendulum Impact Device" employed in this study [28].

types of steel fibres are utilized, as shown in Fig. 2: (1) long straight steel fibre (LSF), length = 13 mm, diameter = 0.2 mm; (2) short straight steel fibre (SSF), length = 6 mm, diameter = 0.16 mm; and (3) hook ended steel fibre (HF) length = 35 mm, diameter = 0.55 mm. The densities of the used materials are shown in Table 1. The oxide compositions of the used cement, limestone powder and nano-silica are presented in Table 2.

2.2. Experimental methodology

2.2.1. Mix design

In this study, based on the approach shown in [21–24,29–31], the modified Andreasen and Andersen model is utilized again to design the sustainable UHPFRC, which is shown as follows [32,33]:

$$P(D) = \frac{D^q - D_{\min}^q}{D_{\max}^q - D_{\min}^q} \tag{1}$$

where D is the particle size (μm), $P(D)$ is the fraction of the total solids smaller than size D, $D_{\max}$ is the maximum particle size (μm), $D_{\min}$ is the minimum particle size (μm) and q is the distribution modulus.

The proportions of each individual material in the mix are adjusted until an optimum fit between the composed mix and the target curve is reached, using an optimization algorithm based on the Least Squares Method (LSM), as presented in Eq. (2). When the deviation between the target curve and the composed mix, expressed by the sum of the squares of the residuals (RSS) at defined particle sizes, is minimized, the composition of the concrete is considered optimal [34].

$$\mathrm{RSS} = \frac{\sum_{i=1}^{n}\left(P_{\mathrm{mix}}\left(D_i^{i+1}\right) - P_{\mathrm{tar}}\left(D_i^{i+1}\right)\right)^2}{n} \tag{2}$$

where P_{mix} is the composed mix, the P_{tar} is the target grading calculated from Eq. (1), and n is the number of points (between $D_{\min}$ and $D_{\max}$) used to calculate the deviation.

As commonly known, the quality of the curve fit is assessed by the coefficient of determination (R^2), since it gives a value for the correlation between the grading of the target curve and the composed mix. Therefore, the coefficient of determination (R^2) is utilized in this study to obtain the optimized mixture given by:

$$R^2 = 1 - \frac{\sum_{i=1}^{n}\left(P_{\mathrm{mix}}(D_i^{i+1}) - P_{\mathrm{tar}}\left(D_i^{i+1}\right)\right)^2}{\sum_{i=1}^{n}\left(P_{\mathrm{mix}}\left(D_i^{i+1}\right) - \overline{P_{\mathrm{mix}}}\right)^2} \tag{3}$$

where $\overline{P_{\mathrm{mix}}} = \frac{1}{n}\sum_{i=1}^{n} P_{\mathrm{mix}}(D_i^{i+1})$, which represents the mean of the entire distribution.

The concrete recipes are listed in Table 3. It can be noticed that the utilized binder amount is relatively low in this study. In general, the developed concrete mixtures can be divided into two categories: (1) with only straight steel fibres (relatively short); and (2) with hook ended steel fibres (relatively long). The total

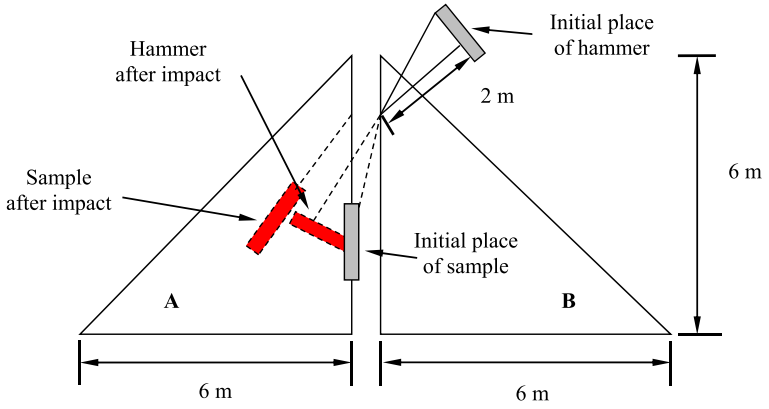

Fig. 6. Working scheme of the "Modified Pendulum Impact Device".

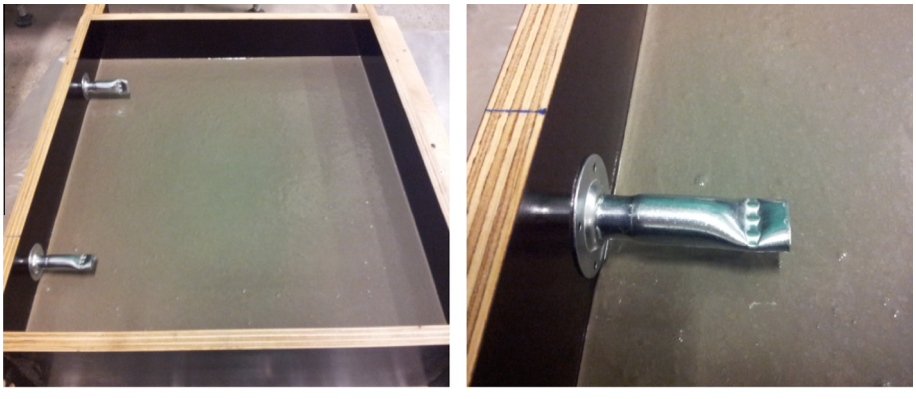

(a) **(b)**

Fig. 7. Fresh sustainable UHPFRC in wooden mould (a) and prepositioned metal inserts in the UHPFRC slabs (b).

(a) (b)

Fig. 8. Constructed hammer, (a) hammer head; and (b) hammer arm in the set-up.

(a) (b)

Fig. 9. Maximum height of the hammer (a) and the concrete slab central point impacted by the hammer (b).

steel fibre amount is 2% by the volume of concrete for all the mixtures. Due to the dimensions difference between these two types of steel fibres, the size of cast concrete samples are different, which will be clarified in the following content.

2.2.2. Mixing procedure

In this study, the concrete matrix is produced following the method described in [25]. Before the hybrid fibres are added into the concrete mixture, they are pre-mixed together for one minute. The mixing is always executed under laboratory conditions with dried and tempered aggregates and powder materials. The room temperature while mixing and testing is constant, about 21 °C. Based on the results from previous research [21–25], the slump flow of the developed sustainable UHPFRC is about 85 cm, and its compressive strength at 28 days is about 135 MPa.

2.2.3. Dynamic performance evaluation

Considering the effect of different fibres on the sample dimensions, two pendulum impact set-ups are employed here: one is "Charpy Impact Device", and the other one is "Modified Pendulum Impact Device".

The "Charpy Impact Device" (as shown in Fig. 3) is employed to test the energy dissipation capacity of the sustainable UHPFRC with only straight steel fibres (No. 2–6 in Table 3), referencing the ASTM E23 [26]. Its maximum kinetic energy output is 147.1 J. The dimension of specimen and the configuration of the loading for the Charpy impact test are presented in Fig. 4, following [27]. After curing in water for 28 days, the hardened samples are prepared for the impact test. After embedding the specimen, the pendulum is released from a height H_1 and swings through the specimen to a height H_2, as shown in Fig. 3(b). Assuming a negligible friction and aerodynamic drag (about 1% of the total impact energy), the energy absorbed by the specimen is equal to the height difference multiplied by the weight of the pendulum. During the testing, at least five specimens are tested for each concrete composition.

Fig. 5 illustrates a down-scaled model of the "Modified Pendulum Impact Device" designed by Verhagen [28]. In this study, this device is employed to evaluate the energy dissipation capacity of the sustainable UHPFRC with hook ended steel fibres (mixtures No. 7 and 8 in Table 3). The "Modified Pendulum Impact Device" consists of two main parts, assembled together: the sample part ("A" shown in Fig. 6) and the hammer part ("B" shown in Fig. 6). As can be noticed, this set-up is different from the normal pendulum impact device, in which the sample is commonly fixed on the frame. When the sample is fixed on the frame, a large

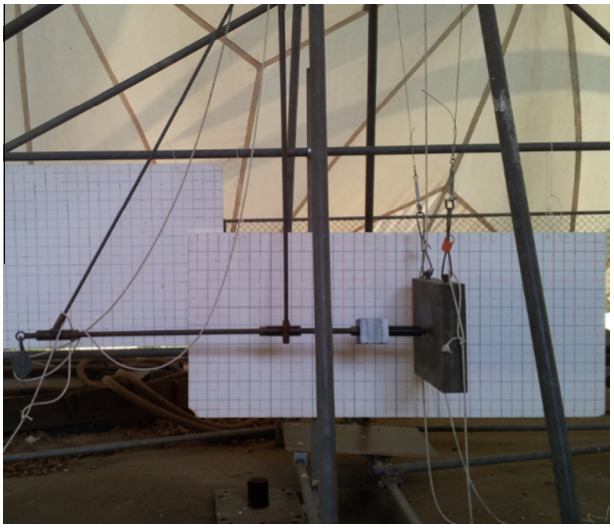

Fig. 10. Meshed board used to calculate all the velocities of hammer and samples.

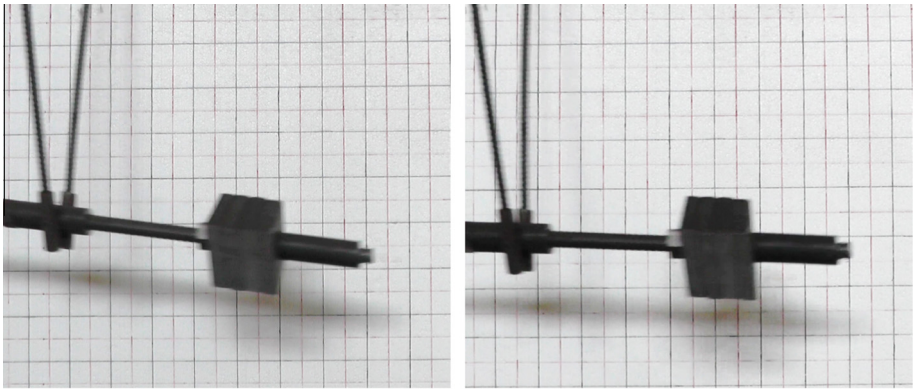

(a) (b)

Fig. 11. Recorded hammer movement during 0.02 s by the used camera.

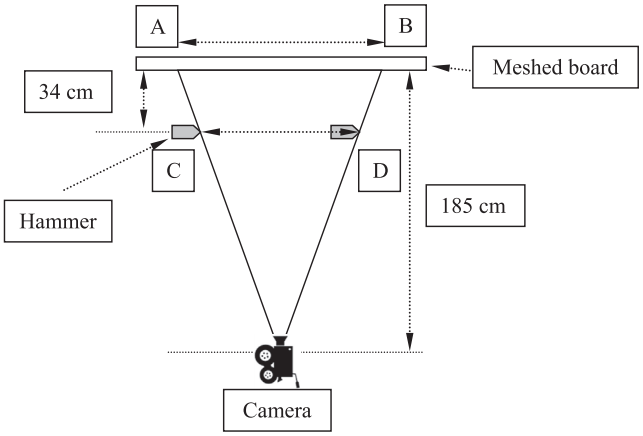

Fig. 12. Relevant mechanisms to calculate the real impact velocity of the hammer.

amount of energy may be consumed by the oscillation of concrete slab and dissipated into the test set-up during the impact process, which limits the test's precision. Hence, in this study, the concrete sample is freely hung on the frame. As shown in Fig. 6, before the impact test, the hammer is firstly lifted to a maximum height (about 3.2 m). Then, it is released from the original height and follows the swing direction to the concrete slab centre. When the hammer swings to the lowest point, it has the highest impact velocity (V_{hammer}). After the impact occurs, the concrete slab will swing away with a velocity V_{slab} and the hammer with a residual velocity ($V_{hammer\text{-}residual}$). Therefore, the energy absorbed by the UHPFRC slab during this impact can be calculated as follows:

$$E_{absorbed} = \frac{1}{2}M_{hammer}V_{hammer}^2 - \frac{1}{2}M_{slab}V_{slab}^2 - \frac{1}{2}M_{hammer}V_{hammer\text{-}residual}^2 \quad (4)$$

where the $E_{absorbed}$ is the absorbed energy by the sustainable UHPFRC slab (J); M_{hammer} and M_{slab} are the masses of impact hammer and concrete slab (kg), respectively; V_{hammer} is the initial impact velocity of the hammer (m/s); V_{slab} is the slab velocity after impact (m/s); $V_{hammer\text{-}residual}$ is the residual velocity of hammer after the impact (m/s).

During the impact process, all the velocities are recorded by a camera. The repeating rebound strikes of the hammer onto the sample are manually avoided in this study. If the UHPFRC slab is not damaged after one impact, then the hammer is released from the original height again, triggering another impact. Until the concrete slab is entirely damaged, the total energy absorbed by the concrete slab can be roughly calculated by adding the absorbed energy in each individual impact:

$$E_{total\text{-}absorbed} = \sum_{1}^{n-1} E_{absorbed} \quad (5)$$

where n represents the strike numbers until the entire damage happens. Due to the fact that the last applied impact can cause the damage of the concrete sample and the velocities of the fragments are difficult to be measured, the absorbed energy from the ultimate impact is not possible to be quantified.

In this study, the fresh concrete is cast in the mould with the size of 500 mm × 500 mm × 100 mm. Two metal inserts are installed on the side of the mould (as shown in Fig. 7), which can help to lift the concrete slab later. The distance between these two metal inserts is 300 mm. To improve the accuracy of the results obtained from the "Modified Pendulum Impact Device" and minimize some potential experimental errors, a series of technical issues should be addressed here. For instance, to flexibly adjust the impact energy, the mass of the hammer should be freely adjustable (Fig. 8a). In addition, considering the fact that it is very important to keep the hammer impacting horizontally on the centre of the target, the location of the added weight should be flexibly adjustable (Fig. 8b). Moreover, during the impact experiments, the distance between the two frames should remain constant. For each impact, the hammer is lifted to the maximum height (about 3.2 m), as shown in Fig. 9a, and the hammer always impacts at the centre of the concrete slab (as shown in Fig. 9b). The velocities of the hammer and the samples are recorded by a camera and calculated with the help of a meshed board (as shown in Fig. 10).

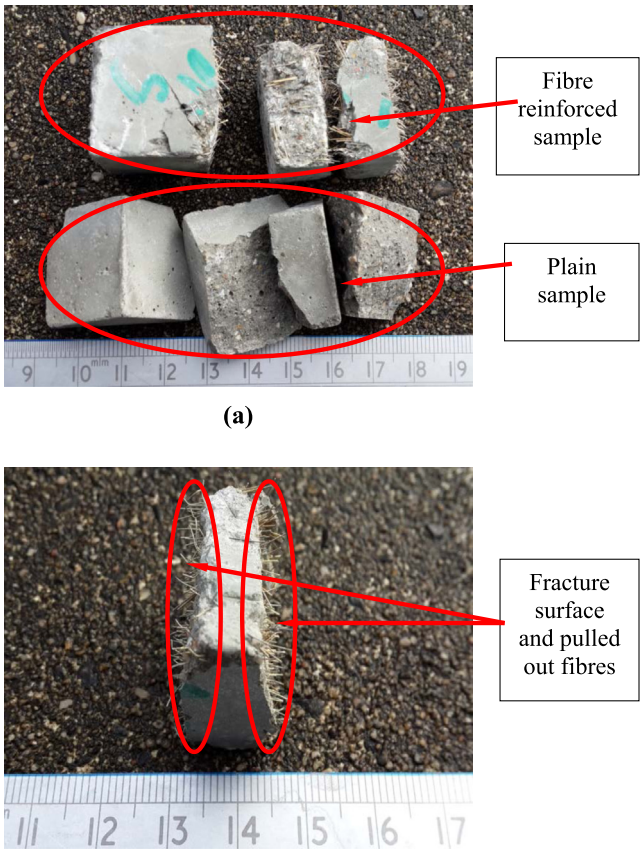

(a)

(b)

Fig. 13. Fractions of the samples after Charpy impact test: (a) comparison of the reinforced and non-reinforced sample after impact loading; and (b) fractured surface of the reinforced sample after impact loading and the pulled out fibres.

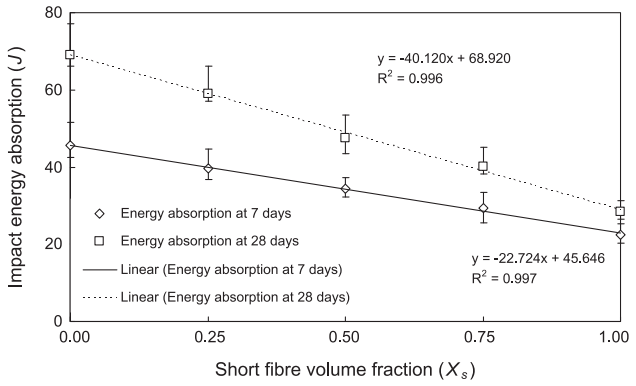

Fig. 14. Variation of the absorbed impact energy of the sustainable UHPFRC with different short fibre volume fractions (X_s), total fibres amount is 2% (vol.).

At the beginning of the tests, the hammer impact velocity is calibrated. As shown in Fig. 11, the time gap between these two pictures is 0.02 s, and the movement of the hammer is about 19 cm. Nevertheless, due to the fact that the used camera cannot be always perpendicular to the impact hammer and there is a gap between the hammer and meshed board, the real movement of the hammer during this 0.02 s should be less than 19 cm. As the mechanism presented in Fig. 12, the hammer movement recorded by the camera is the distance between *A* and *B*, but the real movement of the hammer should be the distance between *C* and *D*. Therefore, based on homothetic triangle theory, it is easy to calculate the real movement of the hammer, which is shown as follows:

$$\frac{D_{CD}}{D_{AB}} = \frac{D_{camera-hammer}}{D_{camera\ -board}} \tag{6}$$

where D_{AB} is the distance between *A* and *B* (as shown in Fig. 12) (cm), D_{CD} is the distance between *C* and *D* (as shown in Fig. 12) (cm), $D_{camera-hammer}$ is the distance between camera and hammer (cm), $D_{camera-board}$ is the distance between the camera and the mesh board (cm).

In this study, the D_{AB}, $D_{camera-hammer}$, and $D_{camera-board}$ are 19 cm, 151 cm and 185 cm, respectively. Hence, the real movement of the hammer (D_{CD}) during the 0.02 s is about 15.5 cm, which means the impact velocity (maximum velocity) of the hammer yields about 7.75 m/s. As mentioned before, the maximum height of the hammer is about 3.2 m and the mass of the hammer is about 40 kg. Hence, assuming that there is no energy consumed in the hammer swing process, the theoretical impact velocity of the hammer can be calculated as:

$$V_{theoretical} = \sqrt{2gh_{hammer}} \tag{7}$$

where $V_{theoretical}$ is the hammer theoretical impact velocity (m/s), g is the gravity of earth constant (9.81 m/s^2) and h_{hammer} is the maximum height of the hammer (about 3.2 m).

Here, the calculated theoretical hammer impact velocity is about 7.92 m/s. Hence, the energy loss during the hammer impact process can be calculated as follows:

$$E_{loss} = \frac{1}{2}M_{hammer}(V^2_{theoretical} - V^2_{tested}) \tag{8}$$

where E_{loss} is the energy loss during the hammer swing process (J), M_{hammer} is the hammer mass (kg), V_{tested} is the tested hammer impact velocity (m/s).

In this research, the energy loss can be attributed to friction, air resistance and frame damping. Based on the equations listed above, the total energy loss amount is estimated at 53.3 J, which is about 4.4% of the initial hammer impact energy. Consequently, it can be stated that then constructed "Modified Pendulum Impact Device" has relatively low energy loss during the impact process and is suitable to be utilized to test the sustainable UHPFRC samples with relatively large dimensions.

3. Experimental results and discussion

3.1. Sustainable UHPFRC under impact from "Charpy Impact Device"

Fig. 13 shows the fractions of the sustainable UHPFRC and reference samples after the Charpy impact test. It can be noticed that the broken sustainable UHPFRC samples are always mainly composed of three cuboid-like fractions, while the fractions of reference sam-

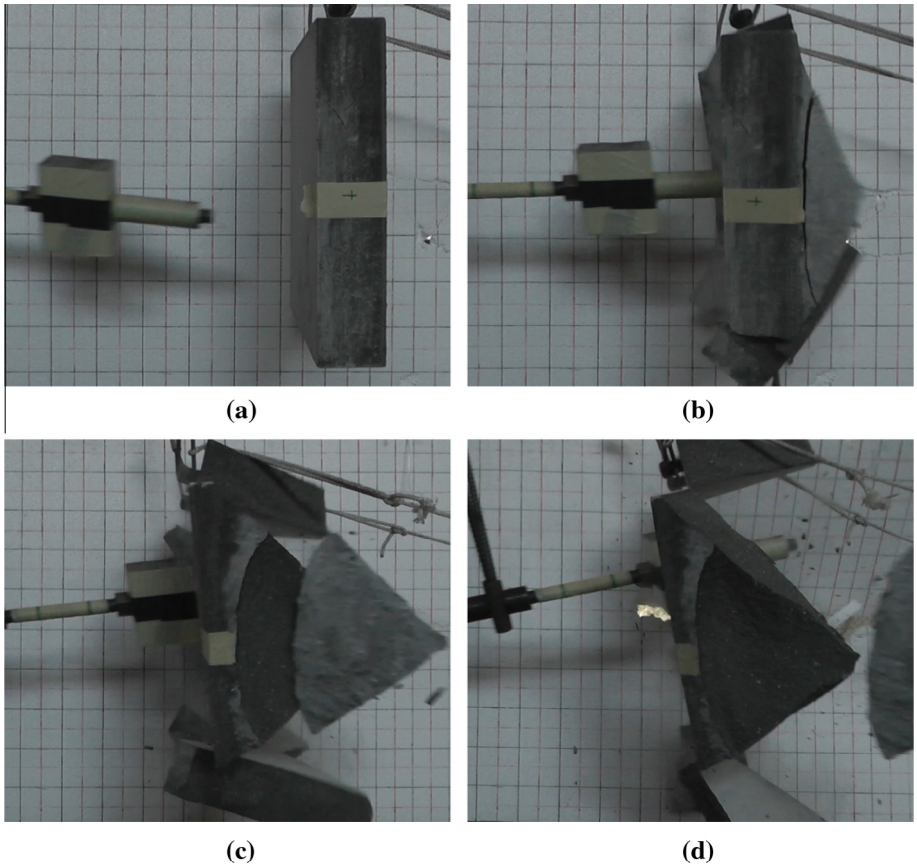

Fig. 15. Dynamic behaviour of UHPFRC matrix (UHPC without fibres) during the first impact.

ples are smaller and more irregular, as shown in Fig. 13(a). Moreover, after the impact loading, not only the concrete matrix of the sustainable UHPFRC sample is destroyed, but also all the embedded steel fibres are pulled out (Fig. 13(b)). Therefore, it can be summarized that the impact energy absorption of the sustainable UHPFRC specimen should mainly include two parts: the energy consumed in breaking the concrete matrix and the energy spent to pull out the fibres embedded in the broken cross sections.

To quantify the energy dissipation capacity of concrete, the variation of the impact energy absorption of the sustainable UHPFRC with different short straight fibre (SSF) volume fractions (X_s, which is defined as the short straight fibre volumetric percentage in the total fibre volume) is investigated, and shown in Fig. 14. As can be noticed, with an increase of the short fibre volume fraction the absorbed impact energy by the sustainable UHPFRC at 7 and 28 days decreases linearly. When the short fibre volume fraction increases from 0 to 1, the impact energy absorption of the sustainable UHPFRC reduces from about 45.6 J and 69.1 J to about 22.3 J and 28.4 J at 7 and 28 days, respectively. Furthermore, the slope of the decreasing line at 28 days is even higher than that at 7 days, which reflects that the addition of short straight fibres (SSF) has a significant effect on the sustainable UHPFRC with relatively high impact energy absorption capacity. Hence, based on the obtained experimental results, it can be concluded that the long straight fibres play a dominant role in improving the energy dissipation capacity of the sustainable UHPFRC. With a constant total steel fibre amount, the increase of short straight fibres content can cause a significant decrease of the energy absorption capacity of the sustainable UHPFRC.

In general, it can be concluded that the long straight fibres are more important than the short straight fibres in improving the energy dissipation capacity of the sustainable UHPFRC. However, for the Charpy impact test, only straight steel fibres are utilized, and the dimensions of the tested samples are relatively small, which is not fully representative for the normal concrete structures in practice. Hence, to further clarify of the dynamic properties of the developed sustainable UHPFRC under pendulum impact, relatively large sized samples (with relatively long steel fibres) should be tested.

3.2. Sustainable UHPFRC under impact from "Modified Pendulum Impact Device"

The energy dissipation capacity of the sustainable UHPFRC with hook ended steel fibres is evaluated by employing the "Modified Pendulum Impact Device". In general, three types of different concrete sample are cast: (1) sustainable UHPFRC matrix without fibres (mixture No. 1 shown in Table 3); (2) sustainable UHPFRC with hybrid steel fibres (mixture No. 7 shown in Table 3); and (3) sustainable UHPFRC with only hook ended steel fibres (mixture No. 8 shown in Table 3). Therefore, based on the dynamic performance of these concrete samples under pendulum impact loadings, it would be possible to assess the effect of different steel fibres categories on the energy dissipation capacity of the sustainable UHPFRC and clearly understand the difference of impact resistance between UHPFRC and UHPC. Here, the dynamic performances of concrete concern the cracks development, absorbed impact energy and fracture morphology of concrete samples.

3.2.1. Cracks development

As shown in the previous sections, the impact energy of the used hammer is about 1200 J. After the first impact, the UHPC

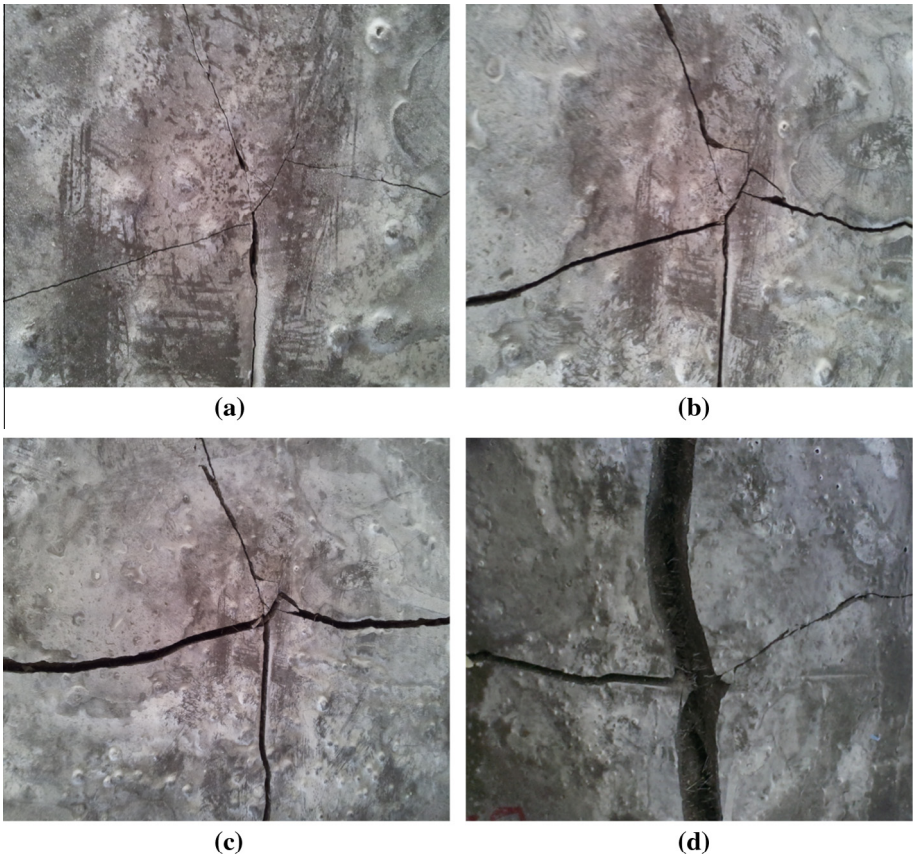

Fig. 16. Cracks development in the sustainable UHPFRC with single sized steel fibres (HF) after each impact: (a), (b), (c) and (d) means the concrete rear surface appearance after the first, second, third and fourth impact, respectively.

(without fibres) has already been seriously damaged (as shown in Fig. 15), which should be attributed to the fact that this concrete is relatively brittle and the cracks growth cannot be well restricted. The cracks are created at the central part of the concrete target and then develop towards the edges. In addition, a clear circular scabbing at the rear surface of the sustainable UHPC can be observed (as shown in Fig. 15b). According to the obtained experimental results, it can be concluded that the energy dissipation capacity of a plain concrete target (without steel fibres) is relatively low. Due to the fact that it is difficult to measure the velocities of all the fragments during the impact process, the absorbed energy by the sustainable UHPC is difficult to be quantified.

Compared to the plain concrete, the developed sustainable UHPFRC with single sized fibres (HF) and hybrid fibres (HF + LSF) shows much better energy dissipation capacity during the pendulum impact tests. Particularly the mixture with hybrid steel fibres, which is damaged after 8 times full impacts, while the one with only hook ended steel fibres (HF) needs 5 times full impact to be destroyed. At the front surface of these two types of concrete, the created crater area is relatively small, and the generated cracks are not easy to be observed after the impact. Nevertheless, at the rear surface of these concrete targets, with the increase of shock numbers, the cracks number and size simultaneously increase. When the embedded steel fibres cannot resist the growth of cracks and hold the concrete slab together, the sustainable UHPFRC target is broken into two pieces. In Figs. 16 and 17, the creation and development of cracks at the rear surface of the sustainable UHPFRC with different fibres after each individual impact are illustrated. As can be observed, after the first impact, some crossed cracks can be noticed at the rear surface of the sustainable UHPFRC with single sized fibres (HF). After the subsequent 3 times impacts, the growth of the created cracks at the concrete rear surface can be

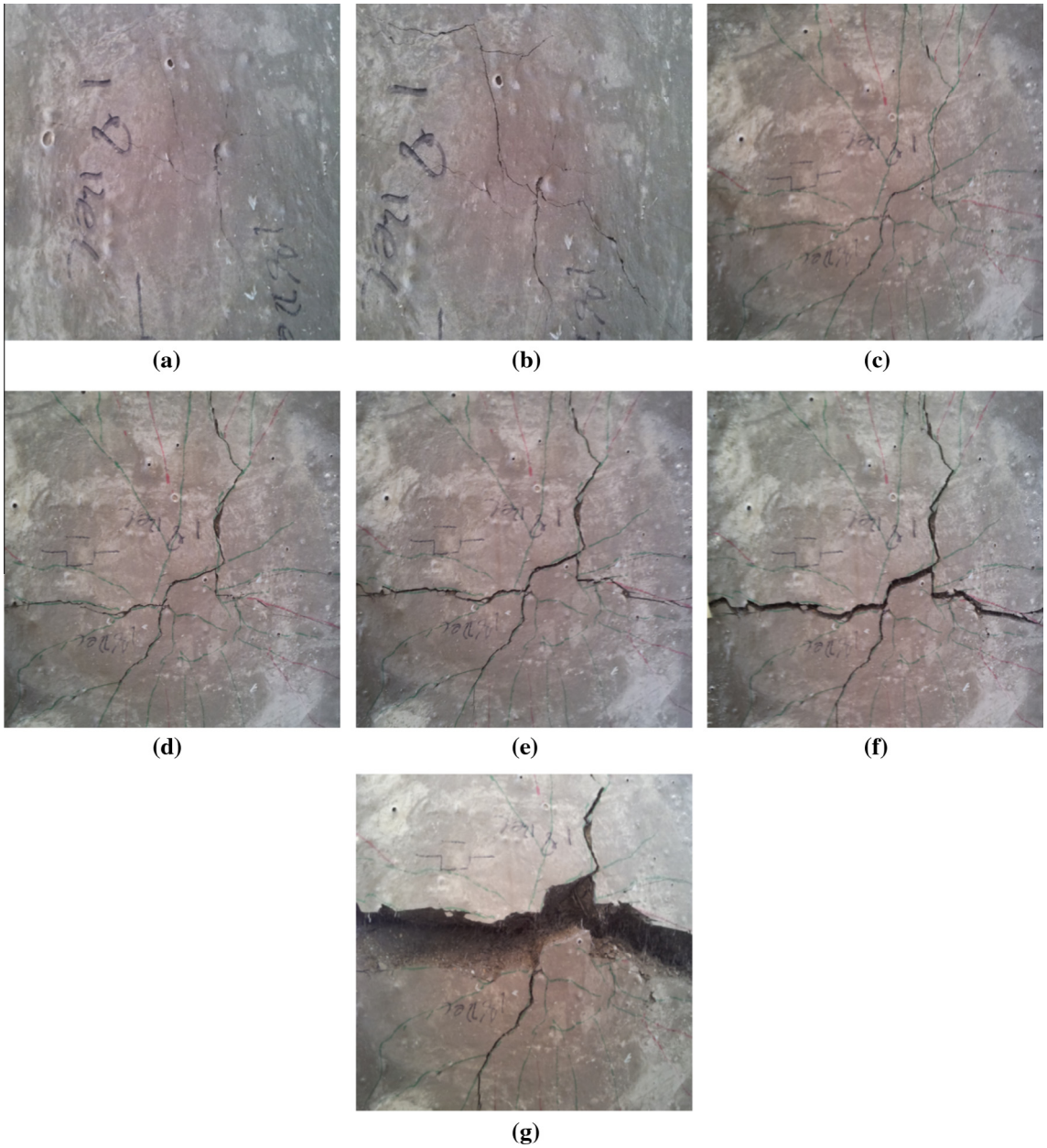

Fig. 17. Cracks development of the sustainable UHPFRC with hybrid steel fibres (HF + LSF) during each impact: (a), (b), (c), (d), (e), (f) and (g) means the concrete rear surface appearance after the first, second, third, fourth, fifth, sixth and seventh impact, respectively.

clearly observed. After the fourth impact, the concrete slab has already seriously bended, but the main concrete parts are still connected by the steel fibres. Similar results can also be noticed in the case of the sustainable UHPFRC with hybrid steel fibres (HF + LSF), in which clear cracks can be found on the concrete rear surface. However, compared to the sustainable UHPFRC with single sized fibres, more cracks can be observed in the mixture with hybrid steel fibres (as shown in Fig. 17f), which is beneficial for improving the energy dissipation capacity of the sustainable UHPFRC.

The phenomena described above can be attributed to the reasons as follows: (1) compared to plain concrete, the addition of steel fibres can well hold the concrete matrix together and restrict the growth of cracks; (2) the short fibres can bridge the micro-cracks while the long fibres are more efficient in preventing the development of macro-cracks, which cause that the stress in the hybrid fibres reinforced concrete can be better distributed; and (3) compared to the sustainable UHPFRC with single sized fibres, more cracks are created in the mixture with hybrid fibres, which means more energy is needed for the growth of cracks. Hence, to better resist the pendulum impact (as shown in this study), the sustainable UHPFRC with hybrid steel fibres is a good choice.

3.2.2. Absorbed impact energy

Based on the results shown in the previous section, it can be concluded that the sustainable UHPFRC with hybrid steel fibres has a better energy dissipation capacity under the pendulum impact than the one with only single sized fibres. To quantify the absorbed impact energy during the impact process, relevant calculations are executed and presented in this section.

As shown in Section 2.2.3, to calculate the energy absorbed by concrete slab, the hammer impact velocity, hammer residual velocity and the concrete target velocity should be measured. With the help of a camera and the meshed board, all these velocities can be computed. One example is shown in Fig. 18. During the 0.02 s time gap, the hammer movement after the impact is about 6 cm, and the concrete slab movement is about 10 cm. Yet, due to the effect of the gap between the hammer and the meshed board (as shown in Fig. 12), the real movements during the 0.02 s are about 4.9 cm and 8.2 cm, for hammer and concrete slab respectively. Therefore, the calculated hammer residual velocity and the concrete slab velocity after the impact are about 2.45 m/s and 4.10 m/s, respectively. Based on Eq. (4), during this impact, the absorbed energy by the concrete target is about 565.3 J, which is about 47% of the total impact energy (1201.3 J).

Afterwards, according to the method shown above and Eq. (5), it is possible to calculate the total energy absorbed amount ($E_{\text{total-absorbed}}$) of the developed sustainable UHPFRC. Nevertheless, due to the fact that it is impossible to calculate the absorbed impact energy of the ultimate impact (when concrete slab is broken into pieces), the obtained $E_{\text{total-absorbed}}$ is the minimum energy absorption capacity of the developed concrete before being seriously defragmented. In this study, the calculated $E_{\text{total-absorbed}}$ values for the sustainable UHPFRC with single sized fibres and hybrid steel fibres are 2248.5 J and 3951.8 J, respectively. These results quantitatively demonstrate that the addition of hybrid steel fibres is beneficial for improving the impact resistance and energy absorption capacity of the developed sustainable UHPFRC.

3.2.3. Fracture morphology

The fracture morphologies of the concrete samples after impact tests are presented in Fig. 19. It can be noticed that the plain concrete (without fibres) is always broken into many pieces,

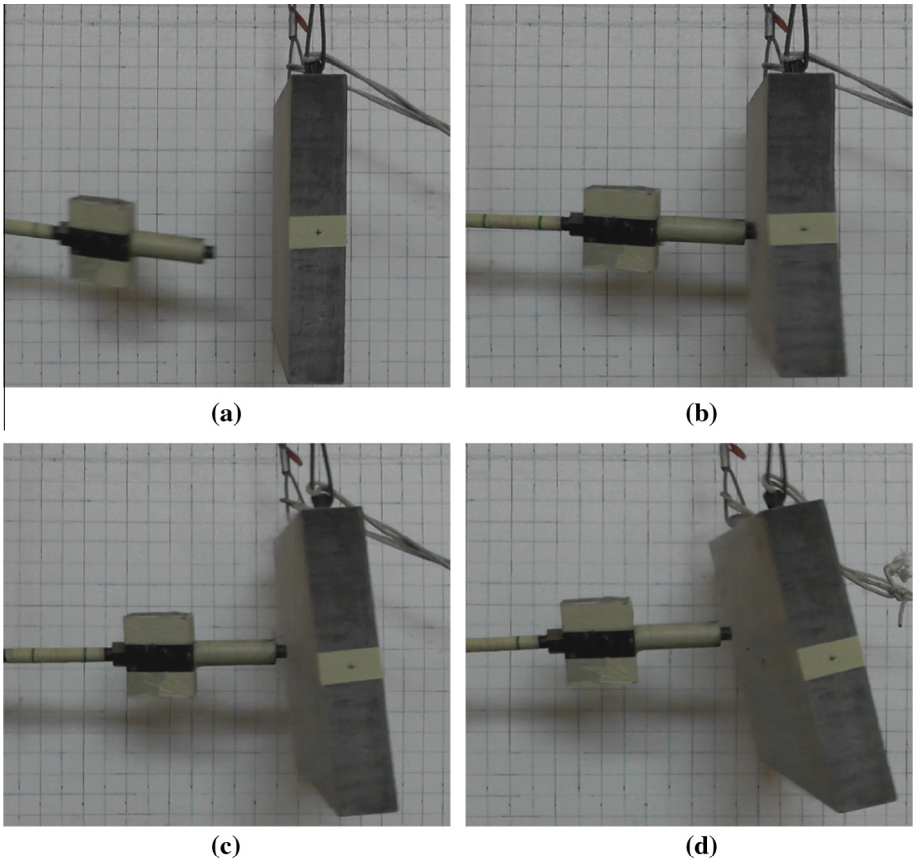

Fig. 18. An example of the impact process recorded by camera.

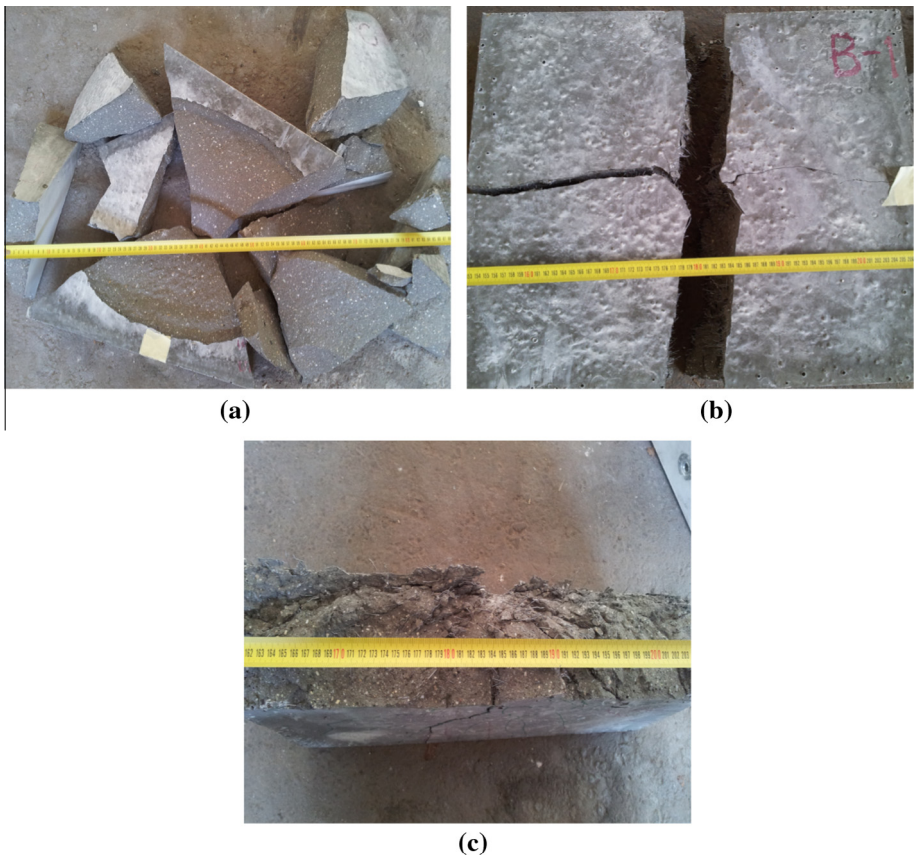

Fig. 19. Fracture morphologies of the designed concrete samples after impact tests: (a) sustainable UHPC matrix (without fibres); (b) sustainable UHPFRC with single sized fibres (HF); (c) sustainable UHPFRC with hybrid fibres (HF + LSF).

while the sustainable UHPFRCs are normally broken into two pieces. This difference can be attributed to the fact that the added steel fibres can well bridge the created cracks during the impact process. With the addition of steel fibres, the cracks growth can be significantly resisted and a large amount of energy is needed to pull the fibres out during the impact process. Particularly when the hybrid steel fibres are included, the stress can be homogeneously distributed and many small cracks are created (as shown in Fig. 19c) under impact loadings, which is positive for improving the energy dissipation capacity of the developed sustainable UHPFRC.

3.3. Comparison of the results obtained from different pendulum impact tests

In this study, two different pendulum impact set-ups have been utilized in the experiments. The dynamic impact test results obtained from "Charpy Impact Device" show that the fibre length plays a dominating role in improving the energy dissipation capacity of the sustainable UHPFRC. With a constant total steel fibre amount, the addition of short fibres decreases the energy absorption capacity of concrete. However, from the results obtained from the "Modified Pendulum Impact Device", it is demonstrated that the addition of hybrid steel fibres is more efficient than single sized fibres in increasing the energy dissipation capacity of the sustainable UHPFRC.

The difference between the obtained results should be mainly attributed to the fibre categories and sample dimensions. As mentioned before, the impact energy absorbed by the sustainable UHPFRC is mainly composed of two parts: the energy used to break the concrete matrix and the energy used to pull out the fibres embedded in the broken cross sections. For the Charpy impact test, due to the fact that the used concrete sample is relatively small and the impact energy is relatively high, all the targets are broken after one time impact (as shown in Fig. 13). Hence, the concrete matrix can be broken immediately, and more energy is consumed in pulling fibres out. Considering the fact that the used SSF is relatively short and easy to be debonded from the concrete matrix, an increase of short fibres (SSF) proportion in the total fibre dosage (2% vol.) can decrease of the energy absorption capacity of the concrete target.

On the contrary, in the case of the tests executed by the "Modified Pendulum Impact Device", the employed sample dimensions are relatively large, which cause that the concrete target cannot be broken after the first impact (as shown in Fig. 17). Therefore, the formation of cracks plays an important role in resisting the impact loadings. Due to the fact that the stress in the hybrid fibres reinforced concrete can be better distributed than that in single sized fibres reinforced concrete, more small cracks are created in the sustainable UHPFRC with hybrid steel fibres, which simultaneously means that more energy is consumed in the formation of cracks and also growth of these cracks. This can be demonstrated by the results shown in Fig. 17, in which the first four times impact mainly causes the creation of cracks and increases the crack numbers. Hence, to effectively apply the sustainable UHPFRC in the production of protective structure, the one with hybrid steel fibres (HF + LSF) is a better choice.

Based on the experimental results obtained here, it can be noticed that the dynamic experimental results of UHPFRC largely depend on the test set-ups and sample dimensions, which implies that there is an urgent request for a systematic standard for evaluating the impact resistance of UHPFRC.

4. Conclusions

This paper addresses the impact resistance of a sustainable UHPFRC under pendulum impact loadings. The modified A&A model is employed for the concrete matrix design, and two pendulum impact set-ups are utilized in the experiments: "Charpy Impact Device" and "Modified Pendulum Impact Device". Based on the obtained results the following conclusions can be drawn:

- For the Charpy impact test, the fibre length plays a dominating role in improving the energy dissipation capacity of the sustainable UHPFRC. With a constant total steel fibre amount (2% vol.), a higher proportion of short fibres (SSF) decreases the energy absorption capacity of the concrete target.
- The results obtained from the "Modified Pendulum Impact Device" demonstrate that the developed sustainable UHPFRC has much better energy dissipation capacity than UHPC (without fibres). In addition, compared to the concrete with single sized fibres (HF), the addition of hybrid steel fibres (HF + LSF) is more beneficial for improving the energy dissipation capacity of the sustainable UHPFRC under pendulum impact.
- The different experimental results obtained from "Charpy Impact Device" and "Modified Pendulum Impact Device" can be attributed to the sample sizes and impact energy. For the Charpy impact test, a large amount of energy is consumed in pulling fibres out, while the creation of cracks plays an important role in resisting the impact for the sample under modified pendulum impact test. Hence, due to the fact the stress in the hybrid fibres reinforced concrete can be better distributed than that in single sized fibres reinforced concrete, the hybrid steel fibres reinforced sample is more efficient in resisting pendulum impact than the concrete with single sized fibres.
- Based on the experimental results obtained here, it can be noticed that the dynamic experimental results of UHPFRC largely depend on the test set-ups and sample dimensions, which implies that there is an urgent need for a systematic standard for evaluating the impact resistance of UHPFRC.

Acknowledgements

The authors wish to express their gratitude to Ing. A.D. Verhagen and G.A.H. Maas for assisting the set-up design and experimental work. Moreover, the appreciation goes to the following sponsors of the Building Materials research group at TU Eindhoven: Graniet-Import Benelux, Kijlstra Betonmortel, Struyk Verwo, Attero, ENCI HeidelbergCement, Provincie Overijssel, Rijkswaterstaat Zee en Delta - District Noord, Van Gansewinkel Minerals, BTE, V.d. Bosch Beton, Selor, Twee "R" Recycling, GMB, Schenk Concrete Consultancy, Geochem Research, Icopal, BN International, Eltomation, Knauf Gips, Hess ACC Systems, Kronos, Joma, CRH Europe Sustainable Concrete Centre, Cement&BetonCentrum, Heros and Inashco (in chronological order of joining).

References

[1] R.P. Kennedy, A review of procedures for the analysis and design of concrete structures to resist missile impact effects, Nucl. Eng. Des. 37 (1976) 183–203.
[2] Q.M. Li, S.R. Reid, H.M. Wen, A.R. Telford, Local impact effects of hard missiles on concrete targets, Int. J. Impact Eng. 32 (2005) 224–284.
[3] B.M. Luccioni, R.D. Ambrosinia, R.F. Danesia, Analysis of building collapse under blast loads, Eng. Struct. 26 (1) (2004) 63–71.
[4] J.R. Clifton, Penetration resistance of concrete: a review, in: Special Publication, National Bureau of Standards, Washington, DC, 1982, pp. 480–485.
[5] A.N. Dancygier, D.Z. Yankelevsky, High strength concrete response to hard projectile impact, Int. J. Impact Eng. 18 (6) (1996) 583–599.
[6] X. Luo, W. Sun, S.Y.N. Chan, Characteristics of high-performance steel fibre-reinforced concrete subject to high velocity impact, Cem. Concr. Res. 30 (6) (2000) 907–914.
[7] V. Bindiganavile, N. Banthia, B. Aarup, Impact response of ultra-high-strength fibre-reinforced cement composite, ACI Mater. J. 99 (2002) 543–548.
[8] M.H. Zhang, M.S.H. Sharif, G. Lu, Impact resistance of high-strength fibre-reinforced concrete, Mag. Concr. Res. 59 (3) (2007) 199–210.
[9] E. Parant, P. Rossi, E. Jacquelin, C. Boulay, Strain rate effect on bending behaviour of new ultra-high-performance cement-based composite, ACI Mater. J. 104 (2007) 458–463.
[10] K. Habel, P. Gauvreau, Response of ultra-high performance fibre reinforced concrete (UHPFRC) to impact and static loading, Cem. Concr. Compos. 30 (10) (2008) 938–946.
[11] J. Lai, W. Sun, Dynamic behaviour and visco-elastic damage model of ultra-high performance cementitious composite, Cem. Concr. Res. 39 (2009) 1044–1051.
[12] P. Richard, M. Cheyrezy, Composition of reactive powder concretes, Cem. Concr. Res. 25 (7) (1995) 1501–1511.
[13] E. Camacho, Dosage optimization and bolted connections for UHPFRC ties, PhD thesis, University Politecnica de Valencia, Valencia, Spain, 2013.
[14] A.S. El-Dieb, Mechanical, durability and microstructural characteristics of ultra-high-strength self-compacting concrete incorporating steel fibres, Mater. Des. 30 (2009) 4286–4292.
[15] A.M.T. Hassan, S.W. Jones, G.H. Mahmud, Experimental test methods to determine the uniaxial tensile and compressive behaviour of ultra-high performance fibre reinforced concrete (UHPFRC), Constr. Build. Mater. 37 (2012) 874–882.
[16] P. Rossi, Influence of fibre geometry and matrix maturity on the mechanical performance of ultra-high-performance cement-based composites, Cem. Concr. Compos. 37 (2013) 246–248.
[17] C. Wu, D.J. Oehlers, M. Rebentrost, J. Leach, A.S. Whittaker, Blast testing of ultra-high performance fibre and FRP-retrofitted concrete slabs, Eng. Struct. 31 (9) (2009) 2060–2069.
[18] P. Máca, R. Sovják, P. Konvalinka, Mix design of UHPFRC and its response to projectile impact, Int. J. Impact Eng. 63 (2014) 158–163.
[19] R. Sovják, T. Vavřiník, J. Zatloukal, P. Máca, T. Mičunek, M. Frydrýn, Resistance of slim UHPFRC targets to projectile impact using in-service bullets, Int. J. Impact Eng. 76 (2015) 166–177.
[20] H. Wu, Q. Fang, X.W. Chen, Z.M. Gong, J.Z. Liu, Projectile penetration of ultra-high performance cement based composites at 510–1320 m/s, Constr. Build. Mater. 74 (2015) 188–200.
[21] R. Yu, P. Spiesz, H.J.H. Brouwers, Mix design and properties assessment of ultra-high performance fibre reinforced concrete (UHPFRC), Cem. Concr. Res. 56 (2014) 29–39.
[22] R. Yu, P. Tang, P. Spiesz, H.J.H. Brouwers, A study of multiple effects of nano-silica and hybrid fibres on the properties of ultra-high performance fibre reinforced concrete (UHPFRC) incorporating waste bottom ash (WBA), Constr. Build. Mater. 60 (2014) 98–110.
[23] R. Yu, P. Spiesz, H.J.H. Brouwers, Effect of nano-silica on the hydration and microstructure development of ultra-high performance concrete (UHPC) with a low binder amount, Constr. Build. Mater. 65 (2014) 140–150.
[24] R. Yu, P. Spiesz, H.J.H. Brouwers, Development of an eco-friendly ultra-high performance concrete (UHPC) with efficient cement and mineral admixtures uses, Cem. Concr. Compos. 55 (2015) 383–394.
[25] R. Yu, P. Spiesz, H.J.H. Brouwers, Development of ultra-high performance fibre reinforced concrete (UHPFRC): towards an efficient application of binders and fibres, Constr. Build. Mater. 79 (2015) 273–282.
[26] ASTM E23, Standard Test Methods for Notched Bar Impact Testing of Metallic Materials, American Society for Testing and Materials, 1992.
[27] B. Xu, H.A. Toutanji, J. Gilbert, Impact resistance of poly (vinyl alcohol) fibre reinforced high-performance organic aggregate cementitious material, Cem. Concr. Res. 40 (2010) 347–351.
[28] A.D. Verhagen, Private communications, discussions and suggestions about the design of the modified pendulum impact device, 2014.
[29] H.J.H. Brouwers, H.J. Radix, Self compacting concrete: theoretical and experimental study, Cem. Concr. Res. 35 (2005) 2116–2136.
[30] G. Hüsken, H.J.H. Brouwers, A new mix design concept for each-moist concrete: a theoretical and experimental study, Cem. Concr. Res. 38 (2008) 1249–1259.
[31] M. Hunger, H.J.H. Brouwers, Flow analysis of water powder mixtures: application to specific surface area and shape factor, Cem. Concr. Compos. 31 (1) (2009) 39–59.
[32] A.H.M. Andreasen, J. Andersen, Über die Beziehungen zwischen Kornabstufungen und Zwischenraum in Produkten aus losen Körnern (mit einigen Experimenten), Kolloid-Zeitschrift 50 (1930) 217–228 (In German).
[33] J.E. Funk, D.R. Dinger, Predictive Process Control of Crowded Particulate Suspensions, Applied to Ceramic Manufacturing, Kluwer Academic Publishers, Boston, the United States, 1994.
[34] G. Hüsken, A multifunctional design approach for sustainable concrete with application to concrete mass products, Ph.D. thesis, Eindhoven University of Technology, Eindhoven, the Netherlands, 2010.